# ASSESSMENT OF STEADY STATE TEARING IN TENSION-DOMINANT CRACK GEOMETRIES

V.P. Naumenko and Yu.D. Skrypnyk
Department of Fracture Modelling, G.S. Pisarenko Institute for Problems of Strength, Kyiv, 01014 Ukraine

ABSTRACT

The paper deals with plane stress tearing in three tension-dominant crack geometries at different in-plane constraint states. Focus is on the initial part of the softening branch of experimental diagrams for centre-cracked specimens fractured under uncontained yielding. It corresponds to the Steady-State Tearing (SST) stage of crack growth in 1.05 mm-thick aluminium plates. The crack extension test data are analysed using a new semi-analytical approach, which is conceptually distinct from the currently used methodology of studying mode I fracture. This approach originates from a purely elastic characterization of the overall response of a crack border to uniaxial and biaxial loading in tension and/or compression. Eventually, three sets of fracture parameters characterizing the SST in differently constrained specimens are contrasted to one another. Some aspects of possible correlation between these parameters and similar parameters associated with the nucleation of a naturally-forming tear crack are outlined in brief terms.

## 1 INTRODUCTION

In-plane constraint is a salient aspect of any approach to assessing the crack extension resistance of thin-walled components under monotonic tensile loading. To predict the critical state of a component in the most credible way, one needs a sufficiently general Transferring Low (TL). This is a common function for data on plane stress tearing in a simple specimen under uniaxial tension and in a complicated component under uniaxial or biaxial loading. In practical terms, a useful TL should allow a reasonable data correlation for a very small specimen (full yielding) and a very large component (globally elastic behaviour) using a minimum number of parameters.

In this context, it is pertinent to outline some methods recently used for assessing the plane stress crack growth in thin aluminium sheets under tensile loading. Specifically, the Gurson-Tvergaard-Needleman and cohesive zone models were applied by Chabanet et al [1] to predict R-curves for a large centre-cracked panel using the data from tensile and Kuhn tear tests. Some experimental evidence presented by Sumpter [2] supports the assumption that the energy dissipation rate under small-scale yielding $D_{ssy}$ is invariant with respect to large amounts of crack growth. Pardoen et al. [3] separated different constituents of the work expended during crack growth in DEN(T) specimens of sheet metals using dimensional considerations.

Finally, two simplified methods are to be mentioned here. A relatively simple and useful application of a cohesive zone model to analysis of plane stress crack growth was reported by Siegmund and Brocks [4]. An extremely simple method of Chausov and Lebedev [5] allows (as the authors state) predicting fracture initiation loads for large-scale panels with a centre crack of different length from data collected in tensile tests of an arbitrary small specimen. The method is very inviting because it eliminates the need for testing specimens with an initial stress raiser and using micromechanically-based damage models and ductile fracture parameters, such as $J$-integral, Crack-Tip Opening Displacement (CTOD), Crack-Tip Opening Angle (CTOA), energy dissipation rate $D$ or essential work of fracture $w_e$.

## 2 GENERAL APPROACH IN OUTLINE

As an alternative to the current approaches, a new way of looking at the formulation of a sufficiently simple and general TL was developed by Naumenko et al. [6-12]. It is based on some

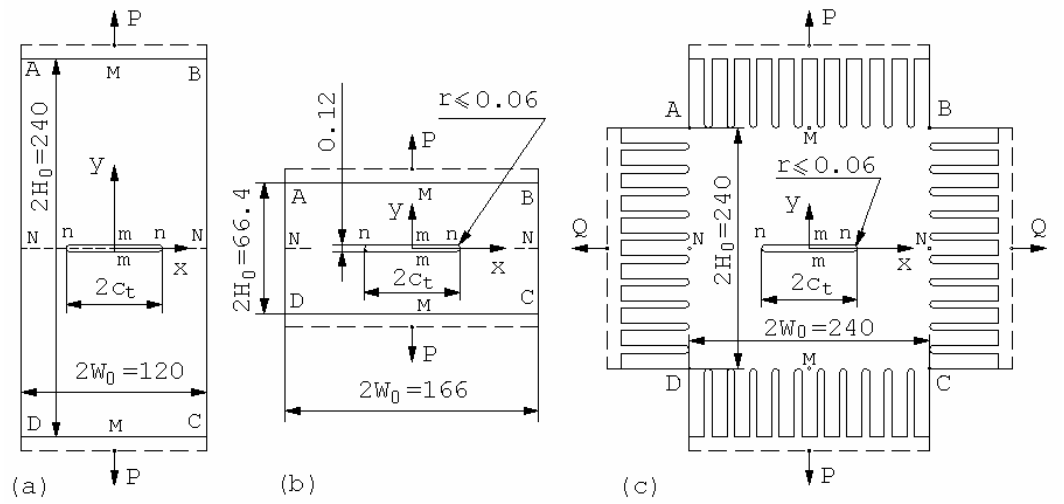


Figure 1: A centre crack in tension-dominant problem domains ABCD of (a) LM(T)-2.0, (b) HM(T)-0.4 and (c) MDEN(T) specimens. All sizes are in mm.

set of interdependent fracture criteria expressed in terms of directly measurable quantities. These are the applied loads, the ratio $k$ of the load $Q$ acting along a crack line to the transverse load $P$, crack-mouth opening displacement and spacing measured between the points $m$ in Fig. 1, crack length and its increments during the SST stage. The input data are collected from the so-called basic tests on two or more identical specimens with original cracks or starting slots of different length. Additional tests of high-constraint specimens of the M(T) configuration without initial stress raisers should be performed in parallel. These tests provide information on mechanical behaviour of the material unaffected by the presence of crack-wake regions. It can potentially be used for the evaluation of the micromechanically-based parameters of Active Damage Zones (ADZ) adjacent to the moving crack tips.

The SST is treated as a quasi-static process of omnidirectional extension of a centre crack cavity of length $2c$, which is represented in fracture analysis by an ideal crack in the form of an elliptic hole having the same length $2c$. It is a continuous process occurring at a constant level of the net-section stress $\sigma_{Ns}$, wherein the increments $2\Delta s$ in the Crack Mouth Opening Spacing (CMOS) $2s$ are in direct proportion to the increments $2\Delta c$ in the crack length $2c$. The CMOS value $2s$ is a sum of non-recoverable component $2s_u$ related to the unloaded state "$u$" and active component, i.e., the crack-mouth opening displacement $2v_m$, induced by the applied loads (Figs. 2 and 3). This semi-analytical concept of stable crack growth taken together with the basic and additional test procedures is called a Unified Methodology (UM) of Mode I fracture investigation.

The main parameters of the UM are the ideal crack tip radius $\rho_0$, the Crack Mouth Opening Angle (CMOA) $\alpha_s = \alpha_{su} + \alpha_{st}$, the Crack Volume Ratio $V_s = V_{su} + V_{st}$, and the specific work of the SST crack growth $A_s = A_{su} + A_{st}$. Of most importance are the active components $\alpha_{st}$, $V_{st}$, and $A_{st}$ of the above parameters characterizing the behaviour of the ADZ under external loading. All fracture parameters depend on the level of the in-plane constraint. For centre-cracked specimens it can be varied by changing the geometry and size of the Problem Domain (PD), initial crack length and amount of crack advance, restraints imposed on the boundaries of the PD, the material deformation behaviour, prior loading history, the load biaxiality ratio $k$, and the magnitude of the applied loads $P$ and $Q$. To simplify the matter as far as possible, we assume that the uniaxial tension testing of the centre-cracked specimens with widely different size ratios $H_0 / W_0$ is the most practical route for assessing the constraint-dependent SST in thin-sheet metals.

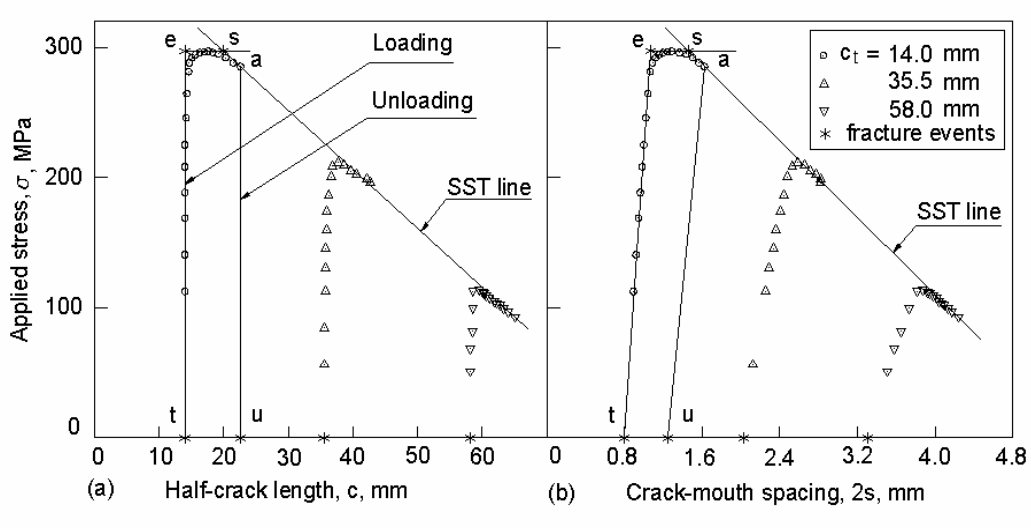


Figure 2: Sequences of test records for three HM(T)-0.4 specimens with tear precracks of lengths 28, 71, and 116 mm. The initial "*t*" and unloaded "*u*" states are shown together with the instant "*a*" of loading interruption and the critical events "*e*" and "*s*".

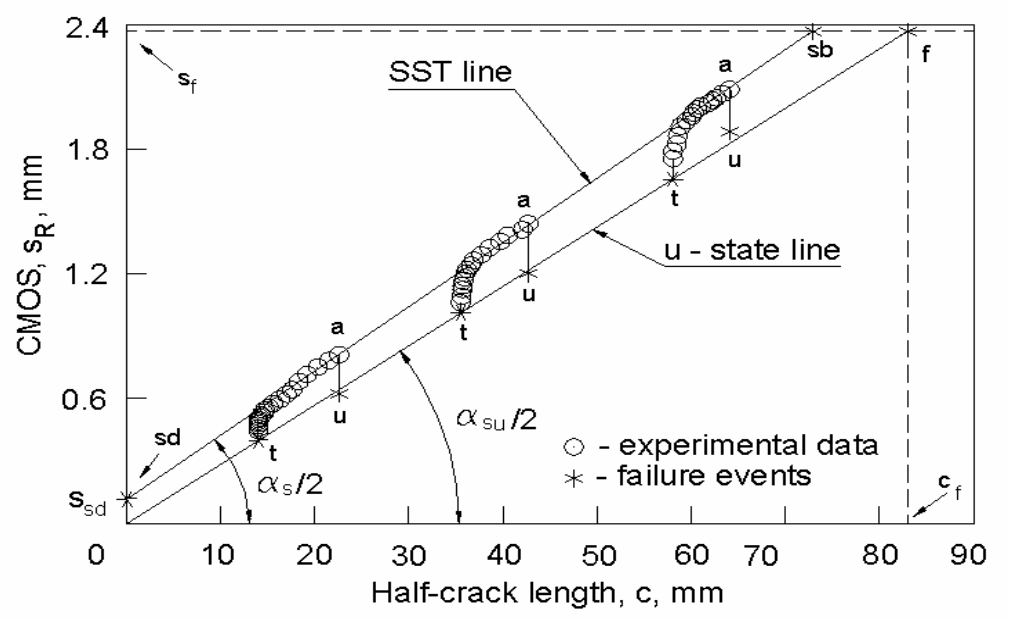


Figure 3: Sequences of $s_R$-curves for three HM(T)-0.4 specimens with tear precracks, which follow from the graphic displays of the test data in Fig. 2 and were plotted assuming that for sufficiently wide specimens in Fig. 1b the final crack length $2c_f \approx 2W_0$.

The UM basic tests were performed on the low-constraint (Fig. 1a) and high-constraint (Fig. 1b) specimens and on cruciform specimens as well. The latter geometry is treated as a physical counterpart of the Typical Structural Element (TSE) usually considered in model descriptions of tension- and/or compression-dominant crack geometries. Sufficiently wide specimens ($2W_0 >> B_0$) are made from one sheet of aluminium alloy 1163 AT having the thickness $B_0$ = 1.05 mm. Its chemical composition and mechanical properties are similar to those of AL 2024-T3. The specimens are stretched by monotonically and slowly increasing the load point displacement $2v_M = 2(H_M - H_0)$ of the rigidly clamped horizontal boundaries of the PD. The initial part of the softening branch of the $P$ vs $c$ and $P$ vs $s$ diagrams (Fig. 2) is represented by two linear segments. This simplification allows us to establish the lower (point "*e*") and upper (point "*s*") boundaries of the instability event "*c*" in a unified manner. Both boundaries are found directly from the raw test data collected on two or more identical specimens containing initial stress raisers of different length $2c_t$. It should be emphasized that a similar initial damage should be introduced in an undeformed and unstressed material of the PDs with original stress raisers of different length.

To determine the spacing $2s$ between the extreme points $m$ on the crack borders, one needs to record a load $P$ versus crack mouth opening displacement $2v_m$ diagram. After a sufficient amount of the post-peak crack growth ($\Delta c > \Delta c_s$ in Fig. 2a) the fracture process should be interrupted at the point "*a*" by monotonic unloading. During the SST stage, the load is related directly to the position of a "moving crack tip," embedded into a fully developed "moving neck," as

$$P = 2 \cdot B_0 \cdot (W_0 - c) \cdot \sigma_{Ns} \quad , \qquad (1)$$

where $\sigma_{Ns} = P_{sc} / 2 \cdot B_0 \cdot W_0$ and $P_{sc}$ is the collapse load depending on the level of in-plane constraint for a given PD without an initial stress raiser. Finally, two experimental diagrams shown in Fig. 2 can be transformed into one (Fig. 3) representing the SST only in terms of the global geometric parameters. Here, the point "*sb*" designates an imaginary transition from the SST stage to the tail-end tearing stage and the point "*f*" the complete loss of load-carrying capacity.

## 3 ACTIVE DAMAGE ZONE PARAMETERS

To correlate parameters of elasticity, plasticity, damage, necking, and cracking, one needs to connect the results of the basic tests with those of the additional tests. The related procedure of the UM can be incorporated in fracture analysis through the notion of a Naturally-Forming Crack (NFC). This term denotes a straight through crack that is freely nucleated in a vicinity of the centre point of a rectangular plate ($x = 0$ and $y = 0$ in Fig. 1) under monotonic tensile loading. In order to experimentally determine the NFC parameters, we performed several tensile tests of high-constraint specimens of the M(T) configuration without initial stress raisers. The most important preliminary observations are as follows: (i) the global necking and subsequent cracking behaviour are separated by the well-defined point "*i*" on the load $P$ versus displacement $2v_m$ diagram, (ii) the difference between the maximum load level $P_{max}$ and the load $P_i$ corresponding to the nucleation of a NFC, as well as between the related $2v_m$ values, is a negligibly small quantity, (iii) the full reduction of the PD width due to cracking $2u_N^{cr} = 2 \cdot (W_{Nf} - W_{Ni})$ is many times smaller than that due to in-plane necking at the instant "*i*", $2u_N^{nc} = 2 \cdot (W_{Ni} - W_0)$ , (iiii) slant fracture of the PD occurs along the $x$ axis in Fig. 1 all the time from the NFC nucleation by shear localization at the instant "*i*" until the complete loss of load-carrying capacity at the instant "*f*" .

These findings indicate that the damage accumulation in a vicinity of the fracture initiation site is a local phenomenon which is possibly independent of the specimen geometry. There is no evidence of distinct discontinuities of the localized necking and cracking processes, of which the traces are usually observed on fracture surfaces [1,3,5]. Both processes appear as to be self-similar

from the instant "*i*" and no visible external evidences of crack-tip blunting can be found on the fracture surfaces. Thus, it is logical to assume that the local strains and stresses in the stationary ADZ without any crack-wake effects and those in the ADZ moving together with the SST crack tip should be, at least, in line. They can be treated as inherent properties of the extremely hardened and damaged material assuming that the crack growth rate effects are negligible.

The lengths of the imaginary NFCs were determined through the use of the critical spacing $2s_{sd}$ obtained from the basic tests (see Fig. 3) and the following relation

$$s_{sd} = 2L_0 \cdot F\left(\frac{L_0}{W_0}\right) \cdot \frac{\sigma_{Ns}}{E}, \qquad (2)$$

where $L_0$ is the effective half-length of the NFC, $L_0 = c_0 + 0.5 \cdot (1-k) \cdot \sqrt{\rho_0 \cdot c_0}$, $c_0$ is the half-length of an equivalent elliptic hole, $F_v(L_0/W_0)$ is the non-dimensional function of the crack-mouth compliance, and $E$ is the elastic modulus. More details on the UM parameters are given in [8-12]. Some parameters of the ADZ adjacent to the moving SST crack tip in the uniaxially loaded specimens and biaxially loaded TSEs are listed in Table 1.

TABLE 1: ADZ Characteristics for SST Crack Growing in AL 1163 AT

| Specimen code and $k$ ratio | Initial stress raiser: type and length, $2c_t$, mm | $s_{sd}$ mm | $\alpha_{st}$ degree | $A_{st}$, MJ/m$^2$ |
|---|---|---|---|---|
| LM(T)-2.0<br>$k = 0$ | Fatigue precracks<br>12.4 – 48.3 | 0.075 | 0.581 | 0.106 |
| HM(T)-0.4<br>$k = 0$ | Starting slots<br>14 – 104 | 0.115 | 0.218 | 0.053 |
| | Tear precracks<br>28 -116 | 0.116 | 0.266 | 0.061 |
| MM(T-TC)<br>$k = 0$<br>$k = 0.5$<br>$k = 1.0$ | Fatigue precracks<br>96<br>96<br>96 | 0.105<br>0.464<br>0.290 | 1.627<br>0.398<br>0.290 | 0.739<br>0.147<br>0.101 |

## 4 SUMMARY

In this work, the global parameters of the ADZ adjacent to the moving crack tip are obtained from the basic tests. None of them can serve as a sufficiently general criterion of attaining the SST stage in the typical structural element whose outer boundaries are nearly free to move under a prescribed value of the load biaxiality ratio $k$. The active components $\alpha_{st}$ and $A_{st}$ of the crack-mouth opening angle $\alpha_s$ and the specific work of fracture $A_s$ are preferable because of their relatively weak sensitivity to prior loading history. Uncoupled from the remote plasticity components $\alpha_{su}$ and $A_{su}$, they can be regarded as the true material properties at a given constraint level. The values of $\alpha_{st}$ and $A_{st}$ determined on high-constraint specimens can provide conservative assessment of the critical states for uniaxially and biaxially loaded centre-cracked plates.

Generally, the results presented support the UM approach to assessing the constraint-dependent crack growth in thin-sheet metals. The uniaxial tensile tests of rectangular plates with the fixed width $2W_0$ and widely different distances $2H_0$ between the rigidly clamped boundaries and the

crack plane are the most practical route to obtain data necessary for formulating a sufficiently simple and general TL. There are reasonable indications that the ADZ parameters deduced from the results of the basic and additional tests may be, at least, in line. Much more work is needed to correlate them through the use of mechanism-based analyses employing a traction-separation law or void-containing cell elements. The self-similarity of necking and cracking processes observed from the very moment of the NFC nucleation should simplify analytical and numerical simulations of crack growth by slant fracture mechanism, i.e., by mixed Mode I and III cracking in the plane inclined at 45º to the loading plane.

**Acknowledgements:** We are grateful to the Science and Technology Centre in Ukraine and the European Union for providing financial support of this work through the STCU project No. 2212.

## 5 REFERENCES

1. Chabanet, O., Steglich, D., Besson, J., Heitmann, V., Hellmann, D., Brocks, W., Predicting Crack Growth Resistance of Aluminium Sheets, *Computational Materials Science*, Vol. 26, pp. 1-12, 2003.
2. Sumpter, J.D.G., The Energy Dissipation Rate Approach to Tearing Instability, *Engineering Fracture Mechanics*, Vol. 71, pp. 17-37, 2004.
3. Pardoen, T., Hachez, F., Marchioni, B., Blyth, P.H., Atkins, A.G., Mode I Fracture of Sheet Metal, *J. Mech. Phys. Solids*, Vol. 52, pp. 423-452, 2004.
4. Siegmund, T. and Brocks, W., Modeling Crack Growth in Thin-Sheet Aluminium Alloys, *Fatigue and Fracture Mechanics: 31st Volume, ASTM STP 1389,* pp. 475-485, 2000.
5. Chausov, N.G. and Lebedev, A.A., Fracture Mechanism in Plastic Materials, *Strength of Materials,* Volume 35, pp.327-333, 2003.
6. Naumenko, V.P., Brittle Fracture and Strength of Materials under Compression and Tension, (in Russian), *Preprint of the Institute for Problems of Srtength,* Kiev, 38 p., 1987.
7. Naumenko, V.P., Modelling of Brittle Fracture in Tension and Compression, In: *Fracture process in Concrete, Rock and Ceramics (RILEM / ESIS),* J.G.M. van Mier, J.G. Rots, and A. Bakker, Eds, London, Vol. 8, pp. 183-192, 1991.
8. Naumenko, V.P., Why and How the Elastic Response of an Ideal Crack is To Be Harmonized with That of an Actual Crack, In: *Proceedings of the Eleven European Conference on Fracture*, edited by M.M. Brown, E.R. de los Rios, K.J. Miller, Sheffield, pp. 1083-1088, 1998.
9. Naumenko, V.P., Volkov, G.S., and Atkins, A.G., Initiation and Propagation of Ductile Tearing: A Search for Biaxial Fracture Criterion, In: *Proceedings of the Sixth International Conference on Biaxial Multiaxial Fatigue and Fracture,* edited by M.M. de Freitas, Lisboa, Vol. II, pp. 975-982, 2001.
10. Naumenko, V.P., Single-Parameter Prediction of Stable Crack Growth in Large-Scale Panels, In: *Proceedings of the Fourteenth European Conference on Fracture*, edited by A. Neimitz, I.V. Rokach, D. Kocanda, K. Golos, EMAS, Sheffield, Vol.2., pp.543-550, 2002.
11. Naumenko, V.P., Volkov, G.S., Assessment of Plane Stress Tearing in Terms of Various Crack Driving Parameters, In: *Proceedings of the Second ASTM-ESIS Conference on Fatigue and Fracture Mechanics, ASTM STP1461*, edited by S.R. Daniewicz, J.C. Newman and K.H. Schwalbe, West Conshohocken, PA, 2003.
12. Naumenko, V.P. and Atkins, A.G., Energy Exchanges During Plane Stress Crack Growth in Uniaxial and Biaxial Tension, In: *Proceedings of the Seventh International Conference on Biaxial/Multiaxial Fatigue and Fracture,* Berlin, 6 pages, 2004.